JACS
JOURNAL OF THE AMERICAN CHEMICAL SOCIETY

Article

pubs.acs.org/JACS

Combining Meyer–Schuster Rearrangement with Aldol and Mannich Reactions: Theoretical Study of the Intermediate Interception Strategy

Marcin Kalek and Fahmi Himo*

Department of Organic Chemistry, Arrhenius Laboratory, Stockholm University, S-106 91 Stockholm, Sweden

Supporting Information

ABSTRACT: Interception of the transient allenyl enolate intermediate of the vanadium-catalyzed Meyer–Schuster rearrangement with aldehydes and imines has been studied computationally using density functional theory. Mechanistic details of the catalytic cycles for each of the reaction variants are established. In particular, it is shown that the active form of the catalyst contains two triphenylsiloxy ligands, the transesterification of vanadate occurs via σ-bond metathesis, and vanadium enolate is directly involved in the key C–C bond formation. The calculations also provide support for the dissociative course of the key 1,3-shift step. The stereochemistry of the reaction is thoroughly investigated, and the obtained energy barriers reproduce and rationalize the experimentally observed (*Z*)-, (*E*)-selectivity. The calculated free energy profiles are analyzed in terms of efficiency of the intermediate enolate interception. It is shown that the investigated reactions represent borderline cases, in which the intermediate trapping is only slightly favored over the undesired isomerization pathway.

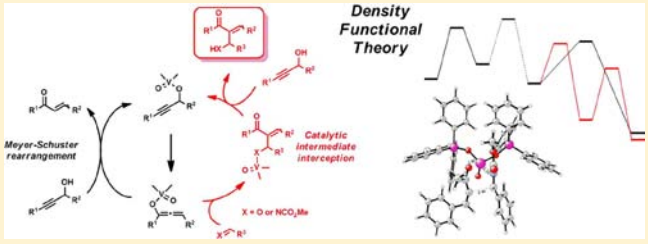

1. INTRODUCTION

The development of new efficient and atom-economical reactions is the main mean of the pursuit of sustainable chemistry.[1] Shortening synthetic routes and maximizing the amount of raw materials that end up in the products lead to reduction in waste generation, which is of increasing importance due to environmental concerns. A good example of an application of these principles is a number of reactions developed by the group of Trost,[2] consisting of vanadium-catalyzed[3] Meyer–Schuster rearrangement[4] combined with aldol- and Mannich-type additions (Scheme 1).

The reactions are classical examples of the catalytic intermediate interception strategy, which relies on diverting the normal reaction pathway (in this case the Meyer–Schuster rearrangement, normally leading to ketone **B**) by trapping the reactive intermediate (allenyl enolate **D**) with an appropriate reagent present in the reaction mixture (aldehyde or imine) that in turn leads to an alternative product (aldol or β-aminoketone, **A**). In general, this strategy opens up the possibility to obtain otherwise inaccessible products, by utilizing often unique chemical reactivities of the transient catalytic intermediates. Additionally, the combination of two reactions can result in synthetically powerful and useful transformations, since it enables the formation of multiple bonds in one-pot reactions. There are several other recent examples of the application of such an approach that illustrate its advantages in terms of achieving unusual selectivities and/or a rapid increase in molecular complexity in a single synthetic step.[5]

The above-mentioned benefits of the intermediate interception approach are clearly demonstrated in the case of the transformation depicted in Scheme 1. Namely, the combination of the two reactions enables a straightforward synthesis of a complex molecular scaffold containing a large concentration of multiple, versatile, and synthetically useful functional groups, starting from relatively simple reactants. Since both the Meyer–Schuster rearrangement and the aldol/Mannich reactions proceed theoretically without the generation of any side-products, the overall transformation is also fully atom-economical. Additionally, due to the special way of the enolate generation, the reaction displays complete regioselectivity, with the C–C bond formation occurring exclusively on the vinylic position and not on the other side of the carbonyl group, as would be expected in an ordinary aldol/Mannich reaction.

The intermediate interception inherently involves an issue of selectivity. In order for this strategy to be successful, the catalytic cycle involving the trapping step must operate more efficiently compared to the normal pathway followed by the catalytic reaction, which is the undesired path under these circumstances. This represents an interesting case from a kinetics point of view and makes the computational approach, based on density functional theory (DFT), a powerful method for investigation of the catalytic intermediate interception. This is due to the fact that the DFT calculations are able to provide detailed free energy profiles for the reactions, which in turn can be analyzed to dissect the sources of selectivity.

Received: August 8, 2012
Published: October 30, 2012

dx.doi.org/10.1021/ja307892c | J. Am. Chem. Soc. 2012, 134, 19159–19169

Scheme 1. General Mechanism for the Combined Vanadium-Catalyzed Meyer–Schuster Rearrangement–Aldol/Mannich Reaction, Involving the Intermediate Interception Strategy

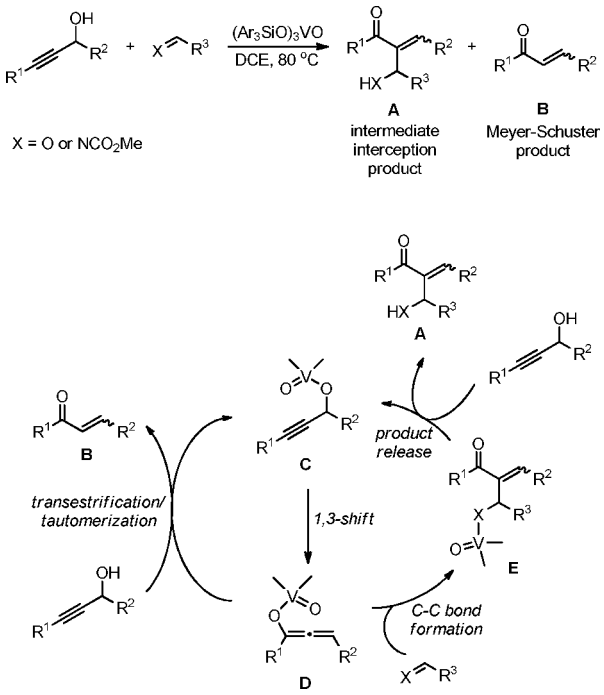

In the present paper, we present a DFT study on the combination of the Meyer–Schuster rearrangement with the aldol and Mannich reactions, with a particular focus on the source of selectivity in the formation of the different possible products. In addition, a number of issues in the mechanism that currently lack a proper understanding are also addressed in the work, such as the structure of the active form of the catalyst, the pathway of the ligand exchange at vanadium center, and the detailed stereochemical course of the reaction.

2. COMPUTATIONAL METHODS

The calculations were performed using the Gaussian09 package[6] and B3LYP functional.[7] Geometries were optimized using the 6-31G(d,p) basis set for C, H, Cl, N, O, and Si, and the LANL2DZ pseudopotential[8] for V. For each stationary point a careful conformational analysis was performed in order to find the conformer with the lowest energy. These were then characterized with frequency calculations to confirm their character as minima (no imaginary frequencies) or transition states (one single imaginary frequency). The final Gibbs free energies reported in this article were obtained from single-point calculations using the larger basis set 6-311+G(2d,2p) for C, H, Cl, N, O, and Si, and LANL2TZ(f) for V, corrected for zero-point and thermal effects at 353.15 K (80 °C, which is the temperature of the experiments) from the frequency calculations, dispersion effect using the B3LYP-D method of Grimme,[9] and solvation free energy. The latter was calculated as a single-point correction on the optimized structures using the conductor-like polarizable continuum model (CPCM)[10] method with the parameters for dichloroethane (DCE), as implemented in Gaussian09.

3. RESULTS AND DISCUSSION

In the first part we describe the investigation of the vanadium-catalyzed Meyer–Schuster rearrangement mechanism alone. Several general issues, such as the structure of the active form of the catalyst (i.e., identity of the two extra ligands on vanadium in Scheme 1) and the mechanism of the ligand exchange at the vanadium center, are addressed here.

In the following two parts, the studies on the Mannich and aldol variants of the reactions are presented. Details of the mechanistic pathways are established first, and then the obtained free energy profiles are combined with the one of the Meyer–Schuster rearrangement and analyzed in order to establish the origins of the overall reaction selectivity. In the case of the Mannich reaction, a modified catalyst had to be used experimentally $[((4\text{-}ClC_6H_4)_3SiO)_3VO$ instead of $(Ph_3SiO)_3VO]$, in order to suppress a side-product formation and achieve high yields. Therefore, the effect of such a catalyst modification on the free energy profile will also be assessed.

There are two stereochemical aspects of the reaction that are pertinent for the investigation. The first one originates from the fact that the propargylic alcohol substrate contains a chiral center. Experimentally, the reactions were carried out using the propargylic alcohol in a racemic form, in turn resulting in the racemic products. Therefore, in this study we will consider all possible diastereomeric transition states and intermediates, assuming a reaction mixture containing both enantiomers of the reactant. For simplicity of the discussion, only the energy of the most stable diastereomer of a given species is reported in the article, whereas the detailed data for the other diastereomers can be found in the Supporting Information. It has also been shown that when enantioenriched reactant was used in the case of the Mannich reaction, formation of a racemic product was observed.[2b] Due to availability of this piece of experimental data, the current computational investigation on the Mannich reaction will be presented before that on the aldol reaction, so that the possible cause of the lack of chirality transfer from the reactant to the final product can be traced.

The second stereochemical aspect of the reaction is the configuration of the double bond in the products. Experimentally, a mixture of (*Z*)- and (*E*)-isomers was obtained during the Meyer–Schuster rearrangement alone,[3] whereas exclusive or preferential formation of (*Z*)-products was observed in the Mannich[2b] and aldol[2a] variants of the reaction, respectively. Therefore, in the present work we will establish the origins of these stereochemical outcomes of the reactions.

3.1. Orthovanadate-Catalyzed Meyer–Schuster Rearrangement. The vanadium-catalyzed Meyer–Schuster rearrangement, contrary to alternative versions of this reaction employing other catalysts, has been a subject of only a very limited number of mechanistic studies.[11] We therefore start our investigation by establishing the details of the catalytic cycle.

In general, in order for the key 1,3-oxygen migration step to occur (**C**→**D** in Scheme 1) the propargylic alkoxide moiety must first be incorporated into the metal complex. Hence, an initial transesterification of the tris(triphenylsilyl) vanadate catalyst **2** with propargylic alcohol **1** needs to take place. There are three triphenylsilanolate groups in **2** that can potentially be substituted with the alkoxide. The calculations show that the incorporation of one, two, or three alkoxide ligands is endergonic by 6.2, 9.6, and 13.6 kcal/mol, respectively (Scheme 2). Hence, the unchanged catalyst **2** is expected to be the dominating vanadium species in the reaction mixture. These data also suggest that the active form of the catalyst most likely contains only a single propargylic alkoxide moiety (**4**), since complexes **5** and **6** are substantially higher in energy. However, in order to definitely exclude the involvement of **5** and **6** in the catalysis, the energies of the corresponding transition states for the 1,3-shift also have to be calculated (see below).

dx.doi.org/10.1021/ja307892c | J. Am. Chem. Soc. 2012, 134, 19159–19169

Scheme 2. Possible Forms of the Vanadium Catalyst Containing Different Numbers of Propargylic Alkoxide Moieties[a]

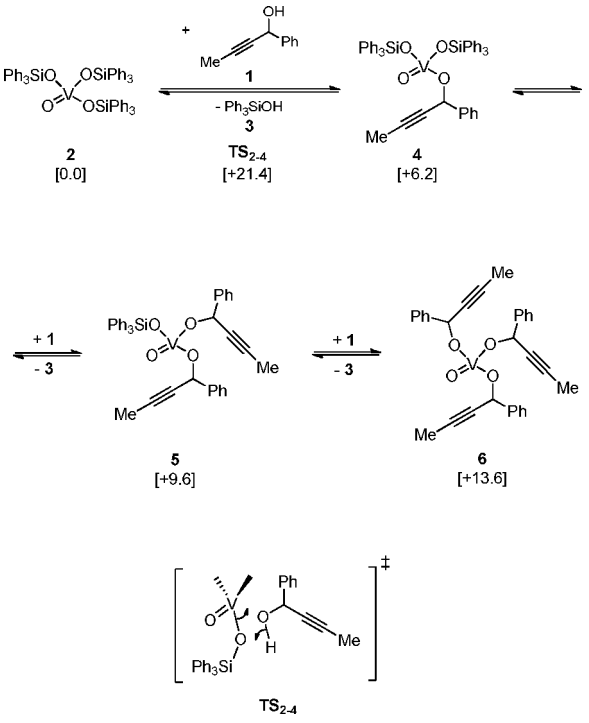

[a]The calculated relative free energies are given in brackets in kcal/mol.

As for the mechanism of the alkoxide ligand exchange at the vanadium center, this process may take place in a concerted or stepwise fashion, the latter with the involvement of a pentacoordinate vanadium intermediates. These possibilities were evaluated computationally in order to establish the pathway via which the catalyst activation process occurs ($\mathbf{TS}_{2-4}$). The calculations show that the five-coordinate vanadium complexes, being the postulated intermediates of the stepwise transesterification pathway, do not correspond to minima on the free energy surface. Instead, during all attempts to optimize the geometry of these species, one of the ligands is spontaneously expelled from the complex. This result is in an agreement with the known preference of vanadium(V) complexes containing bulky ligands, such as the triphenylsilanolate groups in the current system, to adopt a tetracoordinate structure.[12] Therefore, it can be concluded that the stepwise ligand substitution is not a valid transesterification mechanism. Instead, we found a concerted transition state, in which simultaneously with the ligand displacement a proton transfer between the leaving and incoming groups occurs ($\mathbf{TS}_{2-4}$, Figure 1). The energy barrier is calculated to be 21.4 kcal/mol. Such a ligand substitution pathway can in fact be classified as a σ-bond metathesis reaction, which is often found for d^0 metal complexes.[13]

The key step of the vanadium-catalyzed Meyer–Schuster rearrangement is the 1,3-oxygen shift that leads to the formation of the allenyl vanadium enolate intermediate **9** in Scheme 3 (labeled **D** in the general Scheme 1). There are two alternative pathways that the 1,3-shift may follow, resulting in opposite stereochemical outcomes (Scheme 3). The first one is a [3,3]-sigmatropic rearrangement ($\mathbf{TS}_{4-9}$, Figure 2), that would result in a stereospecific transfer of center to axial

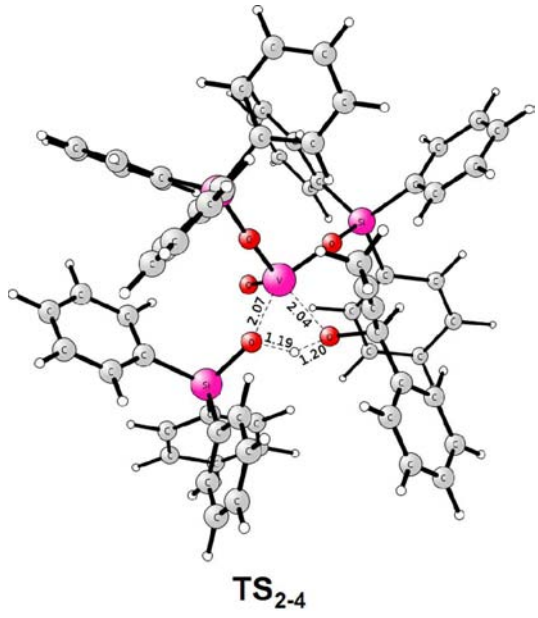

Figure 1. Optimized transition state structure for catalyst activation occurring via a σ-bond metathesis.

Scheme 3. Concerted versus Dissociative Mechanisms for the 1,3-Oxygen Shift

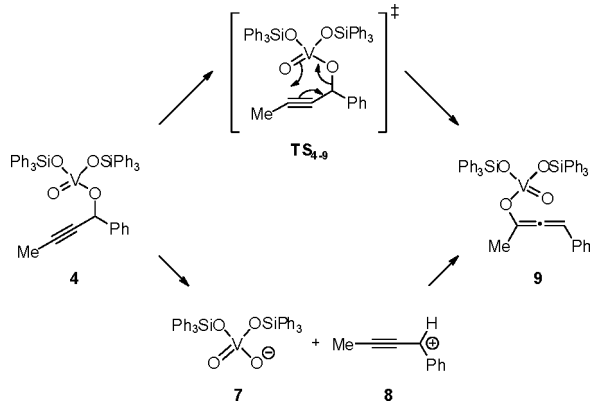

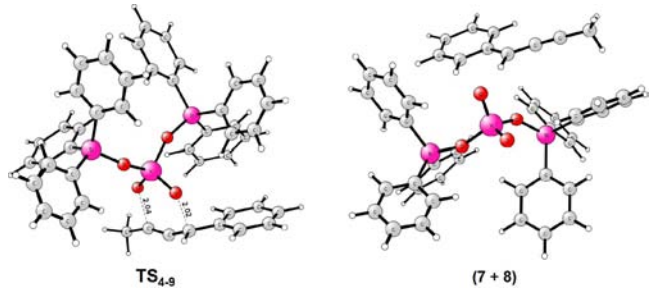

Figure 2. Optimized transition state structure for the 1,3-oxygen shift occurring via a [3,3]-sigmatropic rearrangement and structure of the associated ion pair involved in the dissociative mechanism.

chirality from the propargylic substrate to the allene moiety. The second possibility is a dissociative pathway, proceeding with the intermediacy of vanadate anion **7** and stabilized propargylic cation **8**, whose nonstereospecific recombination would yield **9** without the chirality transfer (i.e., in a racemic form). The latter pathway has been proposed to be responsible for the experimentally observed lack of the chirality transfer

dx.doi.org/10.1021/ja307892c | J. Am. Chem. Soc. 2012, 134, 19159–19169

Scheme 4. Possible Pathways for the Transesterification and Tautomerization of Vanadium Enolate 9 to (*E*)- and (*Z*)-Ketone (11E and 11Z, Respectively)

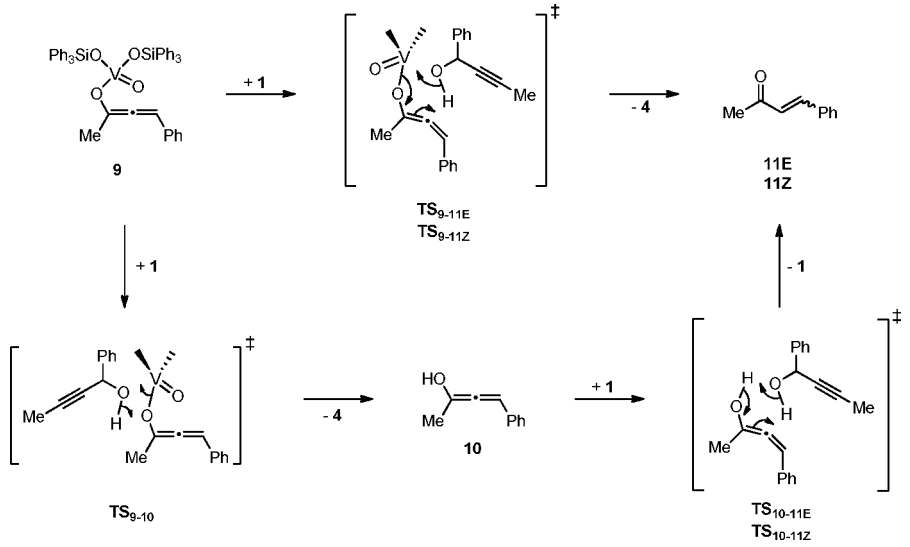

from the propargylic alcohol to the final product during the Mannich variant of the reaction.[2b]

The calculated energy barrier for the concerted 1,3-shift transition state ($\mathbf{TS_{4-9}}$) is 27.4 kcal/mol relative to **2** (for a complete free energy profile of the Meyer−Schuster rearrangement cycle see Figure 4). Calculation of the dissociative mechanism, however, poses a considerable difficulty. It was found that elongation of the C−O bond results only in a rise in the energy, and no energy maximum was detected along this reaction coordinate (see the Supporting Information for details). Hence, the energy of the resulting ion pair **7** + **8** can be considered as the corresponding energy barrier for the dissociative mechanism. Free energy of the dissociated ion pair **7** + **8** was calculated to be 30.2 kcal/mol relative to **2**, that is 2.8 kcal/mol higher than the energy of $\mathbf{TS_{4-9}}$. However, a completely dissociated ion pair does not constitute an appropriate model for the studied reaction, since the ions are not expected to separate completely from each other in the reaction mixture. Additionally, the calculated energy of the dissociated ion pair is prone to be inaccurate, due to deficiencies of the computational methods used when dealing with strongly solvated transient ionic species.[14]

Therefore, an associated ion pair was chosen as both more realistic and computationally more reliable model to estimate the energy barrier for the dissociative mechanism of the 1,3-oxygen shift. However, considering the associated ion pair introduces another difficulty, namely that the two ions may be placed in variable orientations relative to each other. We therefore optimized the associated ion pair starting from several different geometries. The lowest energy structure found is shown in Figure 2 (**7** + **8**), and its free energy was calculated to be 25.0 kcal/mol relative to **2**. The 2.7 kcal/mol difference between the energies of $\mathbf{TS_{4-9}}$ and (**7** + **8**) in favor of the latter indicates that the dissociative pathway is the favored mechanisms for the 1,3-shift. The exact height of the barrier, however, must be treated with caution, as it is expected to contain some inaccuracies, due to the reasons outlined above.

The 1,3-oxygen shifts (via the concerted mechanism) starting from complexes **5** and **6**, containing more than one propargylic alkoxide moieties, were also evaluated and were found to have energies of +32.5 and +39.1 kcal/mol relative to **2**, respectively. This, as pointed out above, implies that **5** and **6** do not contribute to the catalytic activity.

In order to close the Meyer−Schuster rearrangement cycle, the vanadium enolate **9** must undergo a transesterification with propargylic alcohol **1** that regenerates complex **4** and releases free enol **10**. The transesterification ($\mathbf{TS_{9-10}}$, Scheme 4), occurring via a σ-bond metathesis mechanism, was calculated to have a barrier of 19.8 kcal/mol relative to **9**.[15]

Once formed, **10** can undergo a tautomerization to (*E*)- or (*Z*)-ketone (**11E** and **11Z**, Scheme 4), which are low energy products, making this process irreversible (Figure 4). For the tautomerization ($\mathbf{TS_{10-11E}}$ and $\mathbf{TS_{10-11Z}}$) to have a reasonably low barrier, involvement of propargylic alcohol **1** acting as a proton shuttle was found to be necessary. The barriers were calculated to be 19.4 and 23.8 kcal/mol relative to enolate **10**. These results are, however, incompatible with the experimental findings, since the calculated energy difference between $\mathbf{TS_{10-11E}}$ and $\mathbf{TS_{10-11Z}}$ (4.4 kcal/mol) implies that formation of (*E*)-ketone (**11E**) should be noticeably favored over its (*Z*)-counterpart (**11Z**), whereas the actual reaction yields a mixture of the isomers.[3,16]

As an alternative mechanism, we envisioned that the transformation of vanadium enolate **9** could directly produce ketones **11E** and **11Z**, without the intermediacy of free enol **10**. It involves a concerted proton transfer from the incoming alcohol nucleophile, in a six-membered cyclic transition state, directly to the α-carbon atom of the leaving group, with a simultaneous ligand exchange at the vanadium center (Scheme 4). The corresponding transition states ($\mathbf{TS_{9-11E}}$ and $\mathbf{TS_{9-11Z}}$; Figure 3) were found to have lower energies (17.5 and 17.6 kcal/mol, relative to **9**) than those in the pathway via free enol **10**. Additionally, in this case the barriers for the formation of (*Z*)- and (*E*)-ketone are almost identical, which is now consistent with the experimentally observed formation of mixture of the products.[17]

The complete catalytic cycle for the vanadium-catalyzed Meyer−Schuster rearrangement, as established by the calculations, is depicted in Scheme 5, and the corresponding free energy profile is shown in Figure 4. The active form of the catalyst contains two triphenylsilanolate ligands coordinated to the metal center. Importantly, the 6.2 kcal/mol difference in

dx.doi.org/10.1021/ja307892c | J. Am. Chem. Soc. 2012, 134, 19159−19169

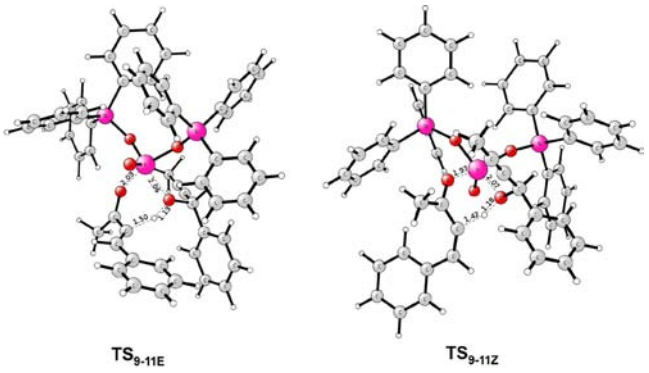

Figure 3. Optimized transition state structures for the concerted transesterification/tautomerization of vanadium enolate **9** to ketones **11E** and **11Z**.

Scheme 5. Summary of the Vanadium-Catalyzed Meyer–Schuster Rearrangement Mechanism

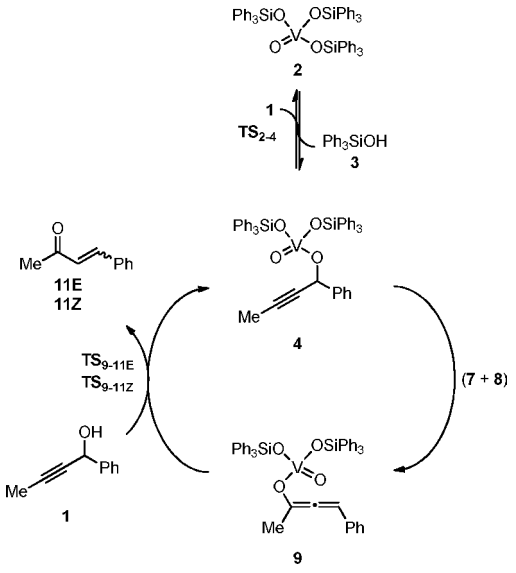

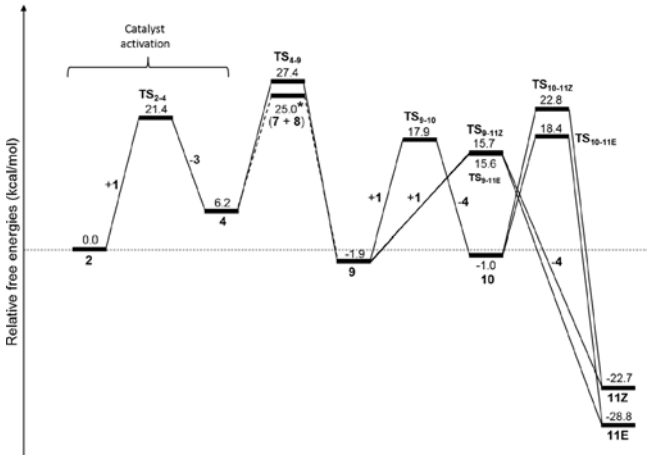

Figure 4. Free energy profile for the vanadium-catalyzed Meyer–Schuster rearrangement. The energy of (7 + 8), indicated with an asterisk, is expected to have a somewhat lower accuracy than the other energies, see text for discussion.

energy between **2** and **4** indicates that, during the reaction, the majority of vanadium remains in an inactive resting state outside the catalytic cycle. The activation of the catalyst ($\mathbf{TS}_{2-4}$), as well as the other ligand exchange processes (transesterifications) in the catalytic cycle, were found to take place via σ-bond metathesis steps, i.e., concerted ligand displacement with a simultaneous proton transfer.

As for the key 1,3-oxygen shift, the calculations indicate that the dissociative pathway should be favored over the concerted one. This implies that intermediate **9** is always formed in a racemic form, even if enantiopure alcohol **1** is used in the reaction. Since **2** and **4** are in equilibrium, the whole energy span between **2** and (7 + 8) (25.0 kcal/mol) is determining for the rate of the 1,3-oxygen shift. This is the largest span among all the barriers in the catalytic cycle; therefore, it is deciding for the turnover frequency (TOF) of the whole rearrangement.

Finally, vanadium enolate **9** reacts irreversibly with propargylic alcohol **1** to regenerate intermediate **4** and yield ketone product **11**. The lowest energy pathway for this transformation was found to involve a 6-membered cyclic transition state ($\mathbf{TS}_{9-11}$). Such a mechanistic route reproduces the experimental findings in terms of the (*E*)/(*Z*) selectivity.

3.2. Mannich Reaction. In the presence of a suitably N-substituted imine (**12**) it is possible for the reaction to diverge from the Meyer–Schuster rearrangement pathway described in the previous section and follow an alternative Mannich route, leading to product **A** in Scheme 1 (X = NCO_2Me). However, it was experimentally found that imine **12** also could undergo an uncatalyzed background reaction with propargylic alcohol **1**, yielding side-product **13** (Scheme 6).[2b] In order to suppress the

Scheme 6. Uncatalyzed Background Side-Reaction Competing with the Mannich Process[a]

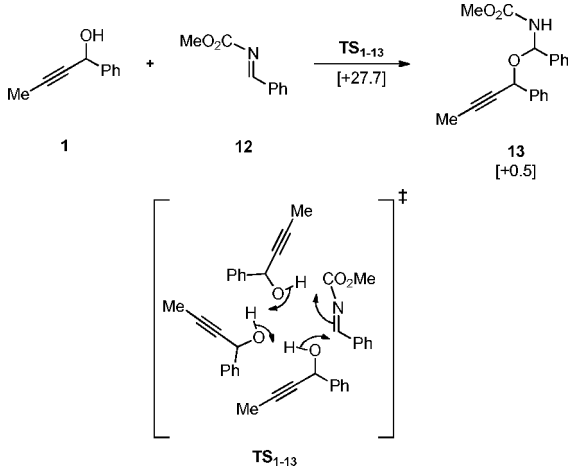

[a]Energies (kcal/mol) relative to (**1** + **12**) are indicated in square brackets.

side-product formation and achieve high yields, a modified catalyst, containing chlorine-substituted aromatic rings [**2-Cl** – $((4\text{-}ClC_6H_4)_3SiO)_3VO)$], had to be used instead of $(Ph_3SiO)_3VO$ (**2**).[2b] Application of **2-Cl** enabled the synthesis of the desired Mannich product, which was obtained as a pure (*Z*)-isomer. It was postulated that the introduction of electron-withdrawing substituents into the catalyst results in the lowering of the barrier for the product release (**E** → **A** + **C** in the general Scheme 1), believed to be the rate-determining step of the reaction.[2b] This should increase the overall reaction rate and make it faster than the background process.

dx.doi.org/10.1021/ja307892c | J. Am. Chem. Soc. 2012, 134, 19159–19169

Scheme 7. Possible Stereochemical Outcomes of the Mannich Reaction Involving the (*R*)-Enantiomer of the Enolate 9R[a]

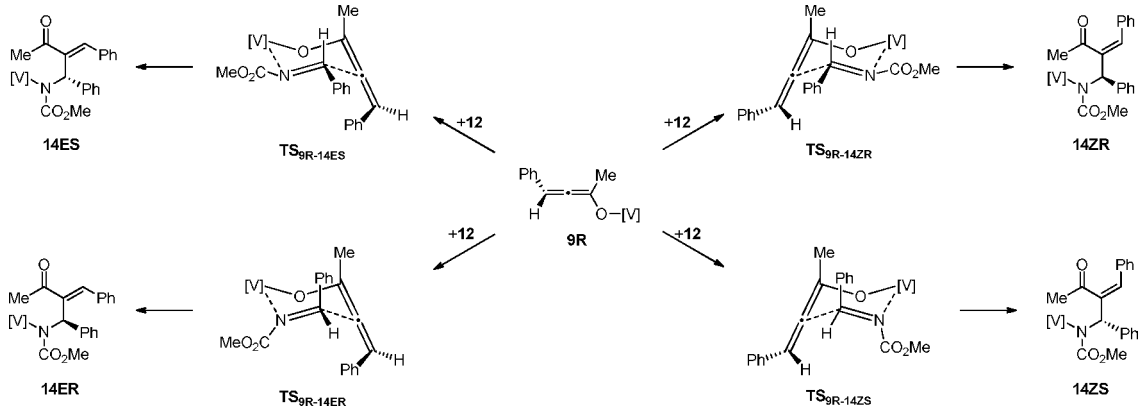

[a]Corresponding scheme for the (*S*)-enantiomer would contain mirror images of all the structures. [V] = $V(O)(OSiPh_3)_2$ or $V(O)(OSi(4\text{-}ClC_6H_4)_3)_2$.

We have first studied the side-reaction depicted in Scheme 6. Computational evaluation of its mechanism showed that the presence of two additional molecules of propargylic alcohol **1**, acting as proton shuttles, is necessary for the transition state ($\mathbf{TS_{1-13}}$) to have a reasonably low energy.[18] Formation of the side-product **13** was found to be practically thermoneutral and requires overcoming a free energy barrier of 27.7 kcal/mol.

The Mannich reaction pathway starts with a C−C bond-forming step occurring via a 6-membered cyclic transition state, in which vanadium enolate **9** attacks the imine **12** with a simultaneous transfer of the vanadium from oxygen to nitrogen.[19] There are two stereochemical aspects of this step that must be considered, namely the (*Z*)-/(*E*)-selectivity and the chirality transfer from the allene moiety to the newly formed stereocenter in the product. Therefore, each enantiomer of enolate **9** can react with the imine in four different ways (hydrogen- or phenyl-substituted face of the enolate with (*Re*)- or (*Si*)-face of the imine, Scheme 7). Since the axial chirality of the allene is still present in the transition states, they are all diastereomers and will thus differ in energy.

We have optimized the transition states for all these possibilities, and the structures are shown in Figure 5. The calculated relative free energies of the transitions states and products of the C−C bond-forming reactions from Scheme 7 are given in Figure 6. In general, transformation of **9** into **14** is highly exergonic and can thus be considered irreversible. Formation of the (*Z*)-products is favored over the (*E*)-counterparts (5.5 kcal/mol difference between $\mathbf{TS_{9R\text{-}14ZR}}$/$\mathbf{TS_{9S\text{-}14ZS}}$ and $\mathbf{TS_{9R\text{-}14ES}}$/$\mathbf{TS_{9S\text{-}14ER}}$). This can be explained by the fact that the approach of the imine in the transition states leading to (*E*)-products is sterically hindered by the phenyl group of the enolate. There is also an energy difference in the pairs of the transition states leading to the different respective enantiomers of **14** (3.7 kcal/mol between $\mathbf{TS_{9R\text{-}14ZR}}$/$\mathbf{TS_{9S\text{-}14ZS}}$ and $\mathbf{TS_{9R\text{-}14ZS}}$/$\mathbf{TS_{9S\text{-}14ZR}}$, and 2.6 kcal/mol between $\mathbf{TS_{9R\text{-}14ES}}$/$\mathbf{TS_{9S\text{-}14ER}}$ and $\mathbf{TS_{9R\text{-}14ER}}$/$\mathbf{TS_{9S\text{-}14ES}}$). This stereodiscrimination between the faces of the imine originates from the presence of a methyl group on one side of the 6-membered ring and is additionally reinforced by the steric bulk of the triphenylsiloxy groups on vanadium.

Overall, from the free energy graph shown in Figure 6 it can be concluded that the C−C bond formation should proceed practically exclusively via transition state $\mathbf{TS_{9R\text{-}14ZR}}$/$\mathbf{TS_{9S\text{-}14ZS}}$, which implies that this step of the mechanism yields **14Z** as the sole product. In addition, the 3.7 kcal/mol difference between the $\mathbf{TS_{9R\text{-}14ZR}}$/$\mathbf{TS_{9S\text{-}14ZS}}$ and $\mathbf{TS_{9R\text{-}14ZS}}$/$\mathbf{TS_{9S\text{-}14ZR}}$ pairs of transition states indicates that practically complete chirality transfer from the preceding enolate **9** is also expected to occur. This however is irrelevant since, as was shown in the previous section, intermediate **9** is formed in a racemic form and hence both enantiomers of **14Z** will be produced in equal amounts.

The Mannich cycle is closed by a ligand exchange at intermediate **14** ($\mathbf{TS_{14-15}}$) that releases the final product **15** and regenerates the active form of catalyst **4** (**E** → **A** + **C** in the general Scheme 1). For the intermediate **14Z** formed in the previous step, this process has a calculated barrier of 21.6 kcal/mol. As shown in Figure 6, this barrier is not the highest one in the catalytic cycle, as suggested previously.[2b] Hence, it is not decisive for the competitive formation of the side-product **13** (Scheme 6).

The overall mechanism of the investigated reaction is shown in Scheme 8, and the corresponding free energy diagram, containing profiles for both the Mannich and Meyer−Schuster reactions catalyzed by $(Ph_3SiO)_3VO$ (**2**), is depicted in Figure 6. The largest energy span in the whole reaction is the one of the 1,3-oxygen shift (25.0 kcal/mol relative to the catalyst resting state **2**). Since it is a common step of the Mannich and Meyer−Schuster cycles, this process constitutes a rate-determining step of the overall reaction, irrespective of the subsequent divergence of the mechanistic pathways. The height of this overall barrier is somewhat lower than the one calculated for the side-reaction shown in Scheme 6 (27.7 kcal/mol, $\mathbf{TS_{1-13}}$). However, to assess the selectivity one must take into account the difference between catalytic and stoichiometric reactions. Experimentally, ≥1 M concentration of **1** and 5 mol % catalyst loading are used,[2b] and such conditions will favor the stoichiometric side-process in the initial stages of the reaction, even though it has a higher barrier. Hence, according to the calculations, overall a mixture of the desired (**15**) and side (**13**) products should be obtained, and this is indeed the observed result with catalyst **2**.[2b]

In order to evaluate the effect of changing the catalyst to $((4\text{-}ClC_6H_4)_3SiO)_3VO$ (**2-Cl**), all the intermediates and transition states from Scheme 8 were reoptimized and their energies recalculated, with the chlorine substituents introduced to the catalyst structure. The obtained free energy profile is depicted in Figure 7. In this case, the overall barrier for the 1,3-shift has decreased to 23.9 kcal/mol, compared to 25.0 kcal/mol before.

dx.doi.org/10.1021/ja307892c | J. Am. Chem. Soc. 2012, 134, 19159−19169

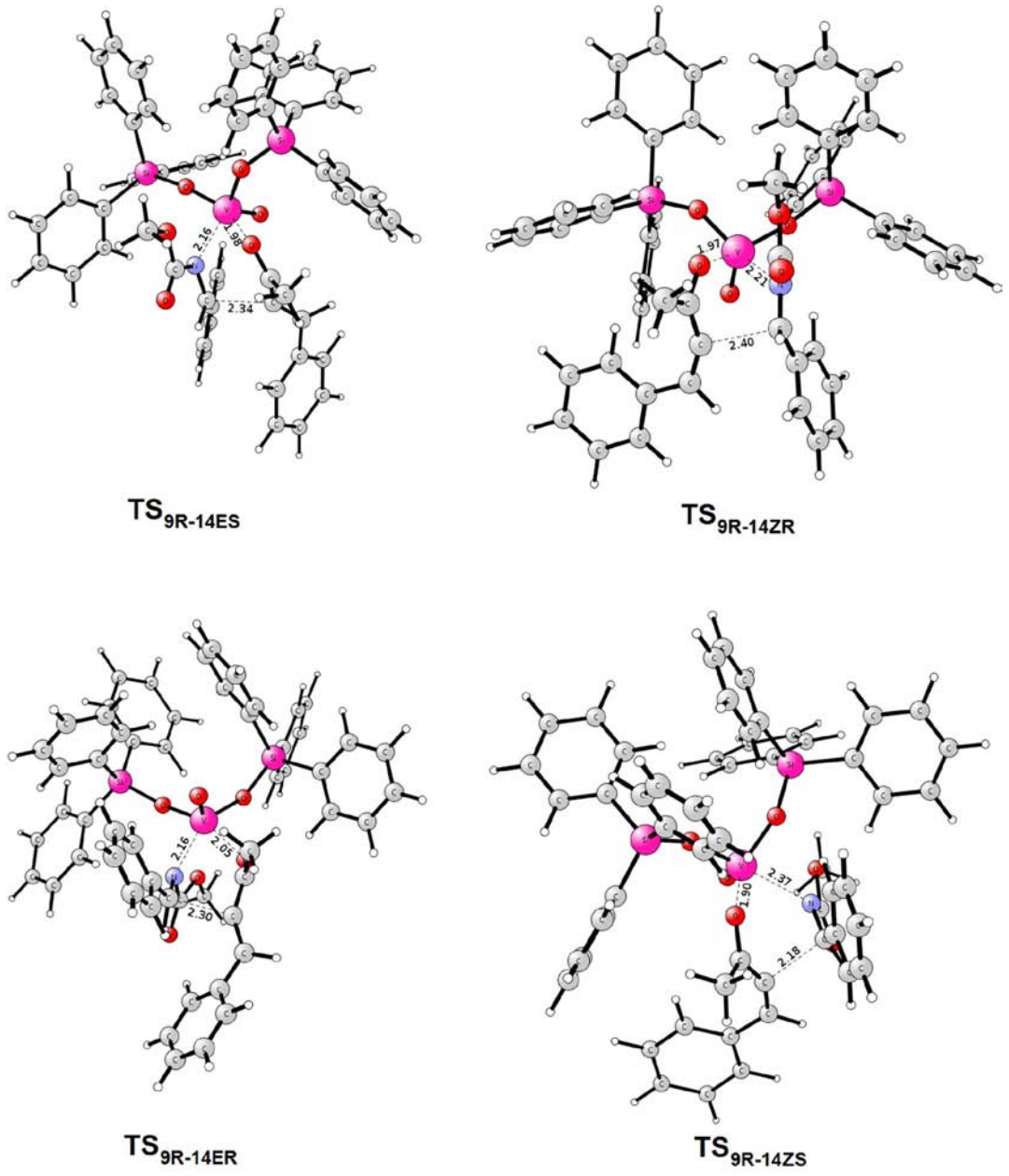

Figure 5. Optimized transition state structures for the C−C bond-formation step of the Mannich reaction.

Hence, with **2-Cl**, the turnover frequency of the catalytic cycle should be almost 10-fold higher than with the unsubstituted catalyst **2**. With such a barrier of the rate-determining step, the vanadium-catalyzed reaction is now even more favored over the background reaction (Scheme 6), which explains the experimentally observed improvement in the **15**/**13** ratio when replacing **2** with **2-Cl** as the catalyst.

The lowering of the energy of (**7-Cl** + **8**) compared to its nonchlorinated counterpart (**7** + **8**) is mainly due to stabilization of (**3-Cl** + **4-Cl**) versus (**1-Cl** + **2**) compared to (**3** + **4**) versus (**1** + **2**) (1.4 kcal/mol). It is difficult to elucidate the exact origin of this effect, since it may arise from both from destabilization of **1-Cl** and/or stabilization of any of **3-Cl** or **4-Cl**, relative to the corresponding nonchlorinated species. The subsequent barrier from **4-Cl** to (**7-Cl** + **8**) is practically the same as the one from **4** to (**7** + **8**) (19.1 and 18.8 kcal/mol, respectively).

The next issue of interest is the selectivity in the formation of the Mannich (**15**) versus Meyer−Schuster (**11**) products. Since both the C−C bond formation ($TS_{9R\text{-}14ZR}$-Cl/$TS_{9S\text{-}14ZS}$-Cl) and transesterification/tautomerization steps (TS_{9-11E}-Cl and TS_{9-11Z}-Cl) are irreversible, the relative energy of the corresponding transition states will determine the selectivity. The calculations show that the energies for the two pathways are very similar. Transition state $TS_{9R\text{-}14ZR}$-Cl/$TS_{9S\text{-}14ZS}$-Cl is only 0.3 kcal/mol lower in energy than TS_{9-11E}-Cl, which indicates that a mixture of products should be observed. This is indeed the case found experimentally, since in order to obtain **15** in a good yield, it was necessary to apply two common laboratory techniques, namely to use an excess (1.2 equiv) of **1** and to perform its slow addition to the reaction mixture.[2b] The former compensates for the inevitable partial transformation of **1** into **11**, while the latter maintains a low level of **1** in the reaction mixture, which in turn decreases the rate of

dx.doi.org/10.1021/ja307892c | J. Am. Chem. Soc. 2012, 134, 19159−19169

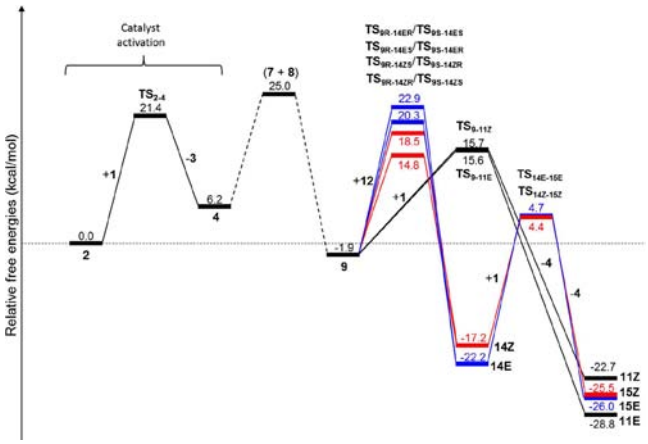

Figure 6. Free energy profile for the Meyer–Schuster rearrangement and the Mannich reaction catalyzed by $(Ph_3SiO)_3VO$ (**2**).

Scheme 8. Summary of the Combined Vanadium-Catalyzed Meyer-Schuster Rearrangement and Mannich Reaction Mechanism

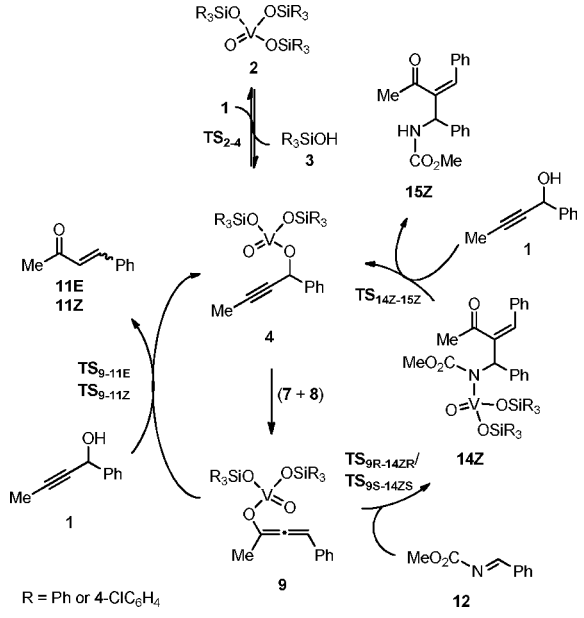

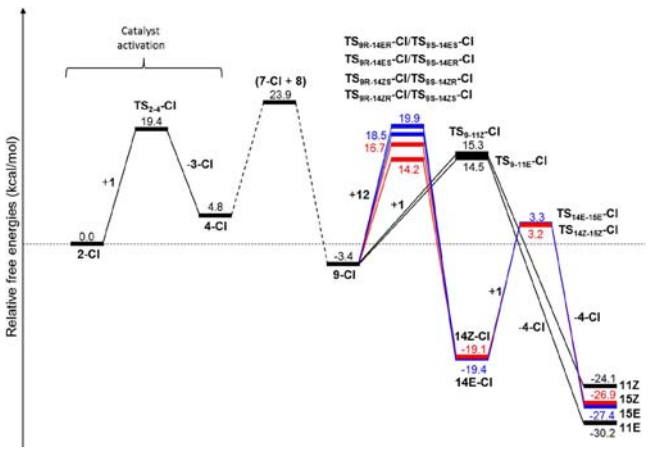

Figure 7. Free energy profile for the Meyer–Schuster rearrangement and the Mannich reaction catalyzed by $((4\text{-}ClC_6H_4)_3SiO)_3VO$ (**2-Cl**).

transesterification/tautomerization (while the rate of the C–C bond formation in the Mannich pathway is unaffected).

The final aspect of the reaction that requires attention is its stereoselectivity. As far as the (*E*)-, (*Z*)-selectivity (**15Z** vs **15E** formation) is concerned, the calculations clearly identify its source in the steric hindrance that the imine encounters when approaching the enolate from the side of the phenyl group (**$TS_{9R\text{-}14ER}$-Cl/$TS_{9S\text{-}14ES}$-Cl** and **$TS_{9R\text{-}14ES}$-Cl/$TS_{9S\text{-}14ER}$-Cl**, Scheme 7), compared to the unhindered approach from the other side, where only the hydrogen atom is present (**$TS_{9R\text{-}14ZR}$-Cl/$TS_{9S\text{-}14ZS}$-Cl** and **$TS_{9R\text{-}14ZS}$-Cl/$TS_{9S\text{-}14ZR}$-Cl**). This effect is manifested in the lower barriers for the formation of **14Z** versus **14E** (17.6 and 20.1 compared to 21.9 and 23.3 kcal/mol, respectively). Hence, according to the calculations the reaction should yield **15Z** practically exclusively, which is in fact the experimentally observed result.

Regarding the lack of chirality transfer from propargylic alcohol **1** to the final Mannich product **15**, the calculations point to the dissociative course of the 1,3-oxygen shift as the reason for the experimentally observed transformation of an enantioenriched alcohol **1** into racemic **15**.[2b]

3.3. Aldol Reaction. The aldol variant of the reaction is mechanistically very similar to the Mannich version presented in the previous section. There are, however, two important differences. First, the aldehyde **16**, contrary to the imine **12** used in the Mannich, does not react in an uncatalyzed background process with the propargylic alcohol. Hence, in this case the standard $(Ph_3SiO)_3VO$ (**2**) catalyst could be successfully used in the experiments. Second, the aldol product is obtained experimentally as a mixture of (*Z*)- and (*E*)-isomers, an aspect that has to be reflected in the calculations.

The C–C bond-forming step of the aldol reaction is analogous to that of the Mannich; i.e. there are four diastereoisomeric transition states possible, similar to those presented in Scheme 7, but containing benzaldehyde **16** instead of the imine.[20] The free energies of these transition states (**TS_{9-17}**, in all the stereoisomeric variants) were calculated and are given in Figure 8. Similarly to the Mannich case, formation of the (*Z*)-isomer of the product (**17Z**) is favored over the (*E*)-isomer (**17E**). The stereodiscrimination between the enantiotopic faces of the aldehyde also occurs (3.3 kcal/mol difference between **$TS_{9R\text{-}17ZS}$/$TS_{9S\text{-}17ZR}$** vs **$TS_{9R\text{-}17ZR}$/$TS_{9S\text{-}17ZS}$**, and 4.8 kcal/mol between **$TS_{9R\text{-}17ES}$/$TS_{9S\text{-}17ER}$** vs **$TS_{9R\text{-}17ER}$/$TS_{9S\text{-}17ES}$**). Hence the axial chirality of vanadium enolate **9** is transferred to

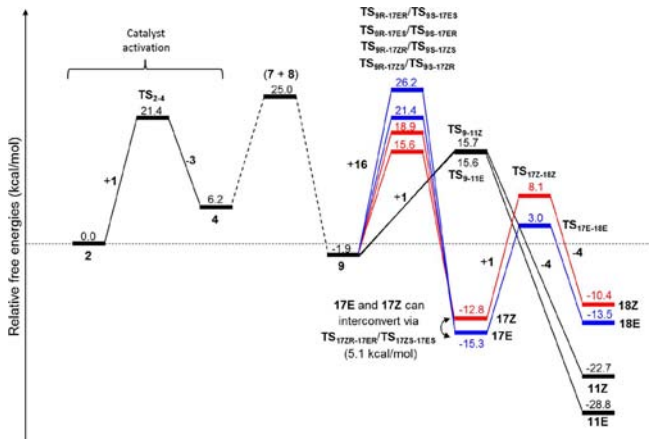

Figure 8. Free energy profile for the vanadium-catalyzed Meyer–Schuster rearrangement and the aldol reaction.

dx.doi.org/10.1021/ja307892c | J. Am. Chem. Soc. 2012, 134, 19159–19169

the asymmetric carbon in alkoxide **17**. This is however irrelevant for the overall reaction stereochemistry, since, as discussed in the previous sections, the preceding 1,3-shift step delivers **9** in a racemic form. Overall, according to the calculations, the C−C bond formation proceeds practically exclusively via $\mathbf{TS_{9R\text{-}17ZS}}$/$\mathbf{TS_{9S\text{-}17ZR}}$, and therefore, **17Z** should be the sole product of this step.

In order to close the catalytic cycle, the vanadium alkoxide **17Z** formed in the C−C bond-formation step must be transesterified with propargylic alcohol **1** to regenerate complex **4** and release the aldol product **18Z**. However, **17Z** is an allylic enolate, and hence, before the ligand exchange takes place, it may undergo a series of 1,3-allylic oxygen shifts.[21] An experimental piece of evidence for such shifts is that when aldehydes other than benzaldehyde were used in the reaction, formation of isomeric products was observed.[2a] In the case of intermediate **17**, however, due to the fact that it contains two identical substituents (phenyl groups), these rearrangements can only affect the stereochemical outcome of the reaction, as presented in Scheme 9.

Scheme 9. Possible 1,3-Allylic Shifts in Intermediate 17[a]

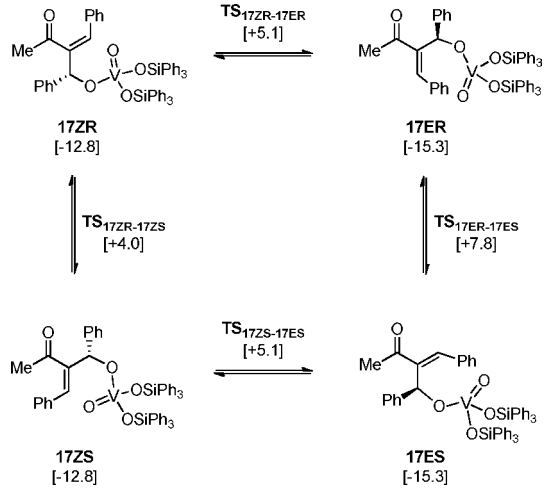

[a]The free energies are given in kcal/mol, relative to complex **2**, i.e., in the same scale as in Figure 8.

Similarly as for the 1,3-oxygen shift being the basis for the Meyer−Schuster rearrangement, we examined both concerted and dissociative 1,3-allylic shifts. In this instance, it was found that the concerted shifts are lower in energy.[22] Hence, intermediate **17** of a given configuration can interconvert both to its enantiomer ($\mathbf{TS_{17ZR\text{-}17ZS}}$ and $\mathbf{TS_{17ER\text{-}17ES}}$, (*Z*)-, (*E*)-configuration maintained) or to a geometric isomer with different arrangement of substituents around the double bond ($\mathbf{TS_{17ZR\text{-}17ER}}$/$\mathbf{TS_{17ZS\text{-}17ES}}$, (*R*)-, (*S*)-configuration maintained). The racemization of **17Z** has the lowest barrier ($\mathbf{TS_{17ZR\text{-}17ZS}}$; 16.8 kcal/mol), followed by **17Z-17E** interconversion ($\mathbf{TS_{17ZR\text{-}17ER}}$/$\mathbf{TS_{17ZS\text{-}17ES}}$; 17.9 and 20.4 kcal/mol, relative to **17Z** and **17E**, respectively), and racemization of **17E** ($\mathbf{TS_{17ER\text{-}17ES}}$; 23.1 kcal/mol). The energy differences between these transition states originate from different, more or less favorable, arrangements of the PhCCCPh backbone (Figure 9). Hence, the barrier required to isomerize **17Z** to **17E** is of a comparable height as that of the transesterification of **17Z** ($\mathbf{TS_{17Z\text{-}18Z}}$, 20.9 kcal/mol). Therefore, although **17Z** is practically the only product of the C−C bond-formation ($\mathbf{TS_{9R\text{-}17ZS}}$/$\mathbf{TS_{9S\text{-}17ZR}}$), its diastereopurity may deteriorate before aldol **18** is eventually released, which explains the experimental observation that the product is a mixture of (*E*)-, (*Z*)-isomers.[2a] Additionally, the racemization of **17Z** occurs readily via $\mathbf{TS_{17ZR\text{-}17ZS}}$, but again, it is irrelevant, since this complex is already formed as a racemate.

The full mechanism of the combined Meyer−Schuster and aldol reaction is depicted in Scheme 10. The only issue that remains to be commented on is the overall selectivity in the formation of aldol **18** versus ketone **11**. Similarly to the case of the Mannich reaction, the first steps of diverging Meyer−Schuster ($\mathbf{TS_{9-11E}}$ and $\mathbf{TS_{9-11Z}}$) and aldol ($\mathbf{TS_{9R\text{-}17ZS}}$/$\mathbf{TS_{9S\text{-}17ZR}}$) pathways are irreversible, and thus, the relative energies of the corresponding transition states are determinant for the selectivity. The calculated energies of $\mathbf{TS_{9-11E}}$ and $\mathbf{TS_{9-11Z}}$ are practically the same as that of $\mathbf{TS_{9R\text{-}17ZS}}$/$\mathbf{TS_{9S\text{-}17ZR}}$. Therefore, a competitive formation of undesired ketone **11** is expected. This indeed is the case experimentally, and in order to obtain aldol product **18** in high yields, an excess of propargylic alcohol had to be used.[2a]

Finally, it is important to point out that the overall rate of the reaction (i.e., the catalytic turnover frequency) is decided at the common step of both cycles, i.e., the 1,3-shift, which has the largest energetic span (25.0 kcal/mol) and constitutes thus the rate-determining step.

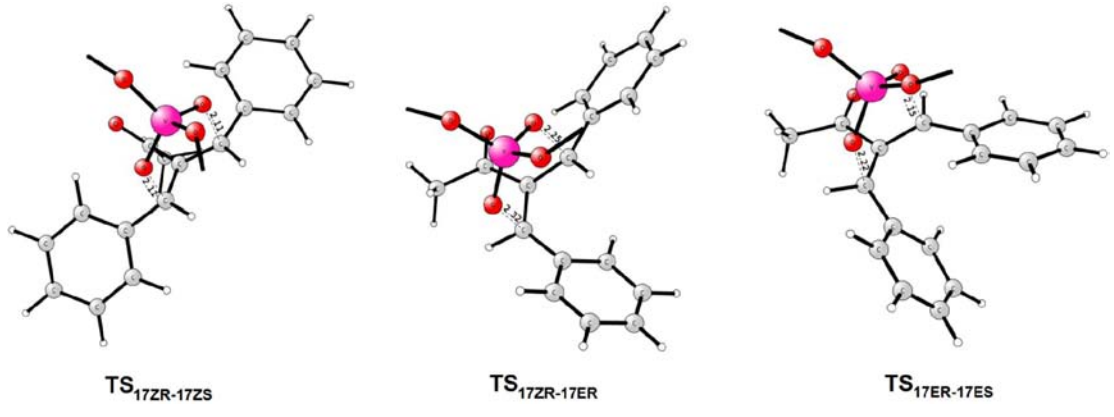

Figure 9. Optimized transition state structures for the 1,3-allylic shifts in intermediate **17**. Note that the triphenylsilane groups are omitted for clarity.

dx.doi.org/10.1021/ja307892c | *J. Am. Chem. Soc.* 2012, 134, 19159−19169

Scheme 10. Summary of the Combined Vanadium-Catalyzed Meyer–Schuster Rearrangement and Aldol Reaction Mechanism

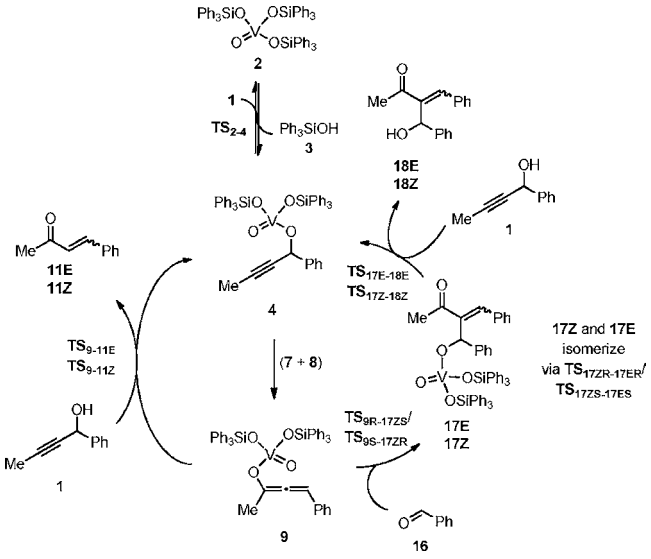

4. CONCLUSIONS

The vanadium-catalyzed reaction involving the intermediate interception strategy was studied in detail by DFT calculations. Plausible catalytic cycles have been established for the vanadium-catalyzed Meyer–Schuster rearrangement, as well as for the aldol and Mannich variants of the tandem transformation. The key mechanistic findings include identification of the active form of the catalyst, determination of the ligand exchange pathway at the vanadium center, and verification of the direct involvement of vanadium enolate in the C–C bond formation. The thorough investigation of the reaction stereoselectivity revealed that the experimentally observed loss of enantiopurity in the Mannich reaction occurs due to the dissociative course of the 1,3-shift. The calculations also provided explanation for the preferential formation of the (*Z*)-isomers of the products, and the partial deterioration of the (*Z*)/(*E*) selectivity in the case of the aldol reaction.

One of the main objectives of the investigation was to examine the selectivity of the reactions with respect to following the two competing branches of the catalytic cycle, i.e., to assess on energetic grounds the efficiency of the intermediate trapping in the studied system. The obtained results demonstrate that, for both the aldol and Mannich versions of the reaction, the trapping is barely energetically favored over the transesterification/tautomerization pathway. Nevertheless it was experimentally possible to carry out these reactions successfully. Hence, these tandem transformations represent borderline cases, which chemically means that, in order to perform other efficient reactions involving the interception of this particular intermediate, use of electrophiles at least as strong as aldehydes or *N*-(methoxycarbonyl)imines is necessary. However, as also seen from the example of the Mannich reaction, one needs to be aware that a problem of side background reactions may arise when using more electrophilic reagents. The presented results provide a general framework for understanding and improving the current reactions as well as for designing new ones based on the interception of allenyl enolate intermediate of the vanadium-catalyzed Meyer–Schuster rearrangement.

■ ASSOCIATED CONTENT

Supporting Information

Complete citation for ref 6, the results of additional calculations not included in the article, the calculated energies and energy corrections for all the species, full list of possible diastereomers of transition states and intermediates with their corresponding relative energies, optimized structures of selected transition states and intermediates, and Cartesian coordinates of all the stationary points. This material is available free of charge via the Internet at http://pubs.acs.org.

■ AUTHOR INFORMATION

Corresponding Author

himo@organ.su.se

Notes

The authors declare no competing financial interest.

■ ACKNOWLEDGMENTS

We acknowledge financial support from The Swedish Research Council (Grants 621-2009-4736 and 622-2009-371) and the Göran Gustafsson Foundations. Computer time was generously provided by the Swedish National Infrastructure for Computing.

■ REFERENCES

(1) Trost, B. M. *Angew. Chem., Int. Ed.* **1995**, *34*, 259–281.
(2) (a) Trost, B. M.; Oi, S. *J. Am. Chem. Soc.* **2001**, *123*, 1230–1231. (b) Trost, B. M.; Chung, C. K. *J. Am. Chem. Soc.* **2006**, *128*, 10358–10359.
(3) Pauling, H.; Andrews, D. A.; Hindley, N. C. *Helv. Chim. Acta* **1976**, *59*, 1233–1243.
(4) Engel, D. A.; Dudley, G. B. *Org. Biomol. Chem.* **2009**, *7*, 4149–4158.
(5) For example: (a) Bartoszewicz, A.; Livendahl, M.; Marítn-Matute, B. *Chem.—Eur. J.* **2008**, *14*, 10547–10550. (b) Shintani, R.; Fu, G. C. *Angew. Chem., Int. Ed.* **2003**, *42*, 4082–4085. (c) Lin, S.; Zhao, G.-L.; Deiana, L.; Sun, J.; Zhang, Q.; Leijonmarck, H.; Córdova, A. *Chem.—Eur. J.* **2010**, *16*, 13930–13934.
(6) Frisch, M. J.; et al. *Gaussian 09, Revision A.02*; Gaussian, Inc.: Wallingford, CT, 2009.
(7) Becke, A. D. *J. Chem. Phys.* **1993**, *98*, 5648–5652.
(8) Hay, P. J.; Wadt, W. R. *J. Chem. Phys.* **1985**, *82*, 270–283.
(9) Grimme, S. *J. Comput. Chem.* **2006**, *27*, 1787–1799.
(10) (a) Barone, V.; Cossi, M. *J. Phys. Chem. A* **1998**, *102*, 1995–2001. (b) Cossi, M.; Rega, N.; Scalmani, G.; Barone, V. *J. Comput. Chem.* **2003**, *24*, 669–681.
(11) Ernan, M. B.; Aul'chenko, I. S.; Kheifits, L. A.; Dulova, V. G.; Novikov, J. N.; Vol'pin, M. E. *Tetrahedron Lett.* **1976**, *17*, 2981–2984.
(12) Crans, D. C.; Smee, J. J.; Gaidamauskas, E.; Yang, L. *Chem. Rev.* **2004**, *104*, 849–902.
(13) Niu, S.; Hall, M. B. *Chem. Rev.* **2000**, *100*, 353–406.
(14) Due to the ionic character, the calculated total solvation energy of the dissociated ion pair **7** + **8** is on the order of 80 kcal/mol. Since the solvation energy is sensitive to the solvent dielectric constant as well as to other parameters used in the CPCM homogeneous model, such a large energy contribution from solvation is a considerable source of error. There is also an additional error originating from the fact that $\mathbf{TS}_{4-9}$ and the associated ion pair (**7** + **8**) are unimolecular, whereas dissociated **7** + **8** is bimolecular. Since the entropic contribution to the free energy, as calculated from the gas phase partition functions, is known to have certain flaws, this also contributes to the overall error when comparing **7** + **8** with $\mathbf{TS}_{4-9}$. We have evaluated the dependency of the energies of $\mathbf{TS}_{4-9}$, **7** + **8**, and (**7** + **8**) on the computational methods used, and the obtained results confirm that indeed the associated ion pair can be considered a more reliable

model for the dissociative course of the 1,3-shift. See the Supporting Information for details.

(15) It has been postulated that **9** can also be transesterified with triphenylsilanol **3**, directly regenerating catalyst **2** instead (see refs 2a and 3). Computational evaluation of this scenario revealed that the appropriate transition state ($\mathbf{TS_{9-10}}$-**3**, see the Supporting Information) has slightly higher energy than $\mathbf{TS_{9-10}}$, and such a pathway should be additionally disfavored due to much lower concentration of **3** compared to **1** in the reaction mixture. Therefore, it will not be considered further here.

(16) Olson, G. L.; Morgan, K. D.; Saucy, G. *Synthesis* **1976**, 25−26.

(17) A similar reaction proceeding via the 6-membered cyclic transition state is also possible with the silanol **3** acting as the nucleophile instead of alcohol **1**, that in turn would yield ketones **11** but accompanied by the catalyst **2** as the products. Appropriate transition states for such a pathway ($\mathbf{TS_{9-11E}}$-**3** and $\mathbf{TS_{9-11Z}}$-**3**, see the Supporting Information) were found computationally to have energies comparable to that of $\mathbf{TS_{10-11}}$, but they should be disfavored due to the lower concentration of **3** compared to **1** in the reaction mixture.

(18) The corresponding transtion states involving one or three molecules of **1** shuttling the proton were found to be higher in energy than $\mathbf{TS_{1-13}}$. See the Supporting Information for details.

(19) There is an additional possibility that the imine reacts with free enol **10**, which has been shown to be an energetically accessible species (via $\mathbf{TS_{9-10}}$, Figure 4). However, calculated barriers for such a mechanistic route show that it is energetically disfavored compared to direct coupling of the imine with the vanadium eneolate **9**. See the Supporting Information for details.

(20) The possibility that the aldehyde reacts with free enol **10** was also considered. Such a mechanism was found to be the lowest energy pathway in a computational study on a related iron-catalyzed isomerization-aldolization of allylic alcohols: Branchadell, V.; Crevisy, C.; Grée, R. *Chem. Eur. J.* **2004**, *10*, 5795−5803. However, in the case of investigated vanadium-catalyzed reaction, it is energetically disfavored compared to direct coupling of the aldehyde with the vanadium enolate **9**. See the Supporting Information for details.

(21) (a) Chabardes, P.; Kuntz, E.; Varagnat, J. *Tetrahedron* **1977**, *33*, 1775−1783. (b) Trost, B. M.; Jonasson, C.; Wuchrer, M. *J. Am. Chem. Soc.* **2001**, *123*, 12736−12737.

(22) The dissociative mechanism of the 1,3-allylic shifts in intermediate **17** was evaluated by calculating the energies of completely dissociated ion pairs of the respective allylic cations (**19EE**, **19ZE**, and **19ZZ**) and vanadate anion **7**. Although, as described above, the dissociated ion pairs are not the most reliable model for the dissociative mechanism, in the case of the 1,3-allylic shifts their energies were found to be 4−7 kcal/mol higher than the energies of the corresponding transition states for the concerted pathway. Such large differences indicate that the concerted pathway is favored in the case of the 1,3-allylic shifts. See the Supporting Information for details.